Diplatinum Complexes Supported by Novel Tetradentate Ligands with Quinoline Functionalities for Tandem C−Cl Activation and Dearomatization

Runyu Tan,[†] Peng Jia,[†] Yingli Rao,[‡] Wenli Jia,[†] Alen Hadzovic,[†] Qing Yu,[†] Xia Li,[†] and Datong Song*[,†]

Davenport Chemical Research Laboratory, Department of Chemistry, University of Toronto, 80 St. George Street, Toronto, Ontario, Canada M5S 3H6, and Chernoff Hall, Department of Chemistry, Queen's University, Kingston, Ontario, Canada K7L 3N6

Received September 14, 2008

Three novel tetradentate ligands with quinoline functionalities, 1,2,4,5-tetrakis(6-ethylquinolin-8-yl)benzene, 1,2,4,5-tetrakis(6-*tert*-butylquinolin-8-yl)benzene, and 1,2,4,5-tetrakis(6-(trifluoromethoxy)quinolin-8-yl)benzene, were synthesized through a three-step protocol and fully characterized by NMR spectroscopic, elemental, and X-ray diffraction analyses. The dinuclear dimethylplatinum(II) complexes of these ligands readily activate C−Cl bonds of $CHCl_3$ at ambient temperature, leading to the formation of the corresponding dinuclear Pt(IV) complex. In these reactions, the central phenyl rings of the tetradentate ligands are reduced to cyclohexadiene dianions and still retain their planarity.

Introduction

The cooperation between multiple metal centers has proven useful in metalloenzymes[1] and heterogeneous catalysis,[2] but it is not as prevalent in the homogeneous systems.[3] Multimetallic catalysis used in homogeneous systems often involves the simple combination of two metal complexes.[3,4] To date, only a few homogeneous catalytic systems are known to use well-defined multinuclear metal catalysts and to have a cooperative effect between multiple metal centers.[3,5] Along the road toward the final goal of efficient multimetallic homogeneous catalysis, knowledge gained from the stoichiometric reactions that demonstrate the cooperative effects between multiple metal centers can be valuable for the rational design of catalytic systems. Previously, a dinuclear platinum complex, Pt_2Me_2(ttab) (ttab = 1,2,4,5-tetrakis(7-azaindol-1-yl)benzene) was reported to cleave C−Cl bonds of $CHCl_3$ at ambient temperature stoichiometrically, owing to the joint action of two metal centers (Scheme 1).[6] In this transformation, the tetradentate ttab ligand was noninnocent, the central phenyl ring of which was jointly reduced into a planar air- and moisture-stable cyclohexadiene dianion by the two platinum centers. This unusual reactivity originates from the unique geometry of Pt_2Me_2(ttab), in which the central phenyl ring of the ttab ligand is situated between the two platinum centers. It is believed to go through a dinuclear Pt(III) intermediate, which is formed from the homolytic cleavage of C−Cl bonds. The two Pt(III) metalloradicals further give up one electron each to the central phenyl ring of the ttab ligand to reduce it into its dianion.

Although this system is not catalytic, it does show the synergism between the two metal centers, as the reduction of benzene into its dianion would otherwise require much harsher conditions.[7] Moreover, if the reaction could be reversed, i.e., reduce $Pt_2Me_2Cl_2$(ttab) back to Pt_2Me_2(ttab), restoring the aromaticity of the central C_6 ring of the ttab ligand and incorporating the Cl into an inorganic salt, a catalytic C−Cl activation could potentially be achieved, which could catalytically degrade chlorinated organics. However, the insolubility of $Pt_2Me_2Cl_2$(ttab) makes the reverse reaction difficult to realize. Despite the limited potential of this system caused by the solubility issue, it is still a unique example of this kind for the facile C−Cl activation and dearomatization of a substituted benzene ring by the joint action of two metal centers under mild conditions.

To generalize this unique reactivity, we have analyzed the geometry of Pt_2Me_2(ttab) to deduce the requirements for the ligand design. The ttab ligand has four rigid 7-azaindol-1-yl groups bonded to the central phenyl ring, so that the nitrogen donor atoms are three bonds away from the central phenyl linker. Such a setting allows the nitrogen lone pairs to point toward the center of the ttab ligand, and thus, the central phenyl ring

* To whom correspondence should be addressed. E-mail: dsong@chem.utoronto.ca.

[†] University of Toronto.

[‡] Queen's University.

(1) Bertini, I.; Gray, H. B.; Stiefel, E. I.; Valentine, J. S. *Biological Inorganic Chemistry, Structure and Reactivity*; University Science Books: Mill Valley, CA, 2007.

(2) (a) Gross, A. *Top. Catal.* **2006**, *37*, 29–39. (b) Liu, S.; Poplaukhin, P.; Ding, E.; Plecnik, C. E.; Chen, X.; Keane, M. A.; Shore, S. G. *J. Alloys Compd.* **2006**, *418*, 21–26. (c) Sinfelt, J. H. *Science* **1977**, *195*, 641–646.

(3) (a) Shibasaki, M.; Yamamoto, Y. *Multimetallic Catalysts in Organic Synthesis*; Wiley-VCH: Weinheim, Germany, 2004. (b) Pignolet, L. H.; Aubart, M. A.; Craighead, K. L.; Gould, R. A. T.; Krogstad, D. A.; Wiley, J. S. *Coord. Chem. Rev.* **1995**, *143*, 219–263. (c) Laneman, S. A.; Stanley, G. G. *Adv. Chem. Ser.* **1992**, *230*, 349–366.

(4) (a) Reed, S. A.; White, M. C. *J. Am. Chem. Soc.* **2008**, *130*, 3316–3318. (b) Li, C.; Chen, L.; Garland, M. *J. Am. Chem. Soc.* **2007**, *129*, 13327–13334. (c) Thiot, C.; Schumtz, M.; Wagner, A.; Mioskowski, C. *Chem. Eur. J.* **2007**, *13*, 8971–8978. (d) Adams, R. D.; Captain, B. *J. Organomet. Chem.* **2004**, *689*, 4521–4529. (e) Ishii, Y.; Miyashita, K.; Kamita, K.; Hidai, M. *J. Am. Chem. Soc.* **1997**, *119*, 6448–6449. (f) Hidai, M.; Fukuoka, A.; Koyasu, Y.; Uchida, Y. *J. Mol. Catal.* **1986**, *35*, 29–37.

(5) (a) Li, H.; Marks, T. J. *Proc. Natl. Acad. Sci. U.S.A.* **2006**, *103*, 15295–15302. (b) Severin, K. *Chem. Eur. J.* **2002**, *8*, 1514–1518.

(6) Song, D.; Sliwowski, K.; Pang, J.; Wang, S. *Organometallics* **2002**, *21*, 4978–4983.

(7) Cassani, M. C.; Gun'ko, Y. K.; Hitchcock, P. B.; Lappert, M. F. *Chem. Commun.* **1996**, 1987–1988.

10.1021/om800893r CCC: $40.75
Publication on Web 11/17/2008

Scheme 1. C−Cl Activation by Pt_2Me_2(ttab)

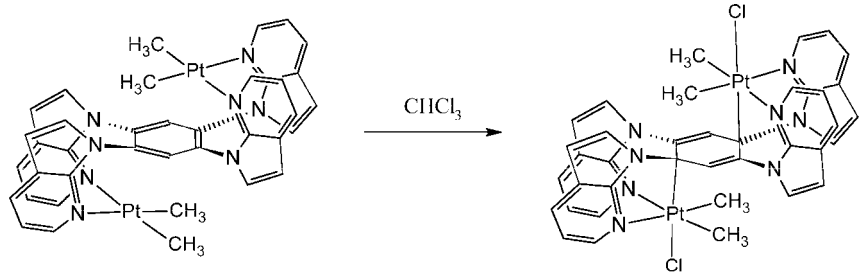

Scheme 2. 8-Quinolinyl versus 7-Azaindol-1-yl

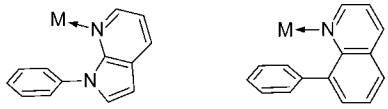

of the ligand is sandwiched between the two square-planar metal centers in the corresponding dinuclear complex.

In our recent research we have chosen 8-quinolinyl as the functional group in the place of the 7-azaindol-1-yl group in ttab to construct new tetradentate ligands, because it has the required rigidity with the nitrogen donor atom three bonds away from the central phenyl ring and the lone pair pointing inward. In addition, it is easy to install functional groups on a quinoline ring, which may potentially improve the solubility of the metal complexes of the ligand. Moreover, quinoline has a six-membered ring fused with a pyridine ring, while 7-azaindole has a five-membered ring fused with a pyridine ring. Therefore, using 8-quinolinyl instead of 7-azaindol-1-yl for the ligand construction will force the metal center to be closer to the central phenyl linker group (Scheme 2). Such a shorter distance may result in higher activity, because the short metal-to-phenyl contact distance appears crucial in the facile C−Cl cleavage reaction.[6] Herein we report the syntheses and characterizations of a series of novel tetradentate ligands featuring 8-quinolinyl functionality and the reactivity of the corresponding dimethylplatinum complexes toward C−Cl activation reactions.

Experimental Section

General Considerations. Unless otherwise stated, all preparations and manipulations were performed in air and all reagents were purchased from commercial sources and used without further purifications. 2-Bromo-4-ethylaniline,[8] 2-bromo-4-*tert*-butylaniline,[8] 2-bromo-4-(trifluoromethoxy)aniline,[8] and $[Pt(CH_3)_2(SMe_2)]_2$[9] were prepared according to the literature procedures. THF solvent for the syntheses of boronic acids was purified using the solvent purification system from Vacuum Atmospheres Co. DMF and water for Suzuki coupling reactions were degassed prior to use. NMR spectra were recorded on a Mercury 300, a Varian 400, or a Bruker Avance 400 spectrometer. Both ^{1}H and ^{13}C NMR spectra were referenced relative to the solvent's residual signals but are reported relative to Me_4Si. Elemental analyses were performed at our chemistry department with a PE 2400 C/H/N/S analyzer.

Synthesis of 8-Bromo-6-ethylquinoline (1a). Sodium 3-nitrobenzenesulfonate (4.5 g, 20 mmol), $FeSO_4 \cdot 7H_2O$ (27.8 mg, 0.1 mmol), boric acid (0.61 g, 10 mmol), 2-bromo-4-ethylaniline (2 g, 10 mmol), and 3.26 mL of concentrated sulfuric acid were mixed in a 250 mL round-bottom flask. The mixture was heated to 150 °C, and glycerol (5.52 g, 60 mmol) was added slowly via a dropping funnel. The reaction mixture was then kept at 150 °C for 4 h, cooled to ambient temperature, neutralized with 10% NaOH solution, and extracted with Et_2O. The organic layers were combined and dried by Na_2SO_4. The solvent was removed under reduced pressure, and the crude product was purified through column chromatography using CH_2Cl_2/hexanes as eluent to give **1a** (1.4 g, 60% yield) as a yellow oil. ^{1}H NMR ($CDCl_3$, 300 MHz, 25 °C): δ 8.99 (dd, ^3J = 4.5 Hz, ^4J = 1.5 Hz, 1H), 8.19 (dd, ^3J = 8.4 Hz, ^4J = 1.5 Hz, 1H), 7.95 (d, ^4J = 2.0 Hz, 1H), 7.57 (s, 1H), 7.43 (dd, ^3J = 4.4 Hz, ^3J = 8.4 Hz, 1H), 2.82 (q, ^3J = 7.5 Hz, 2H), 1.34 (t, ^3J = 7.5 Hz, 3H). ^{13}C NMR ($CDCl_3$, 75 MHz, 25 °C): δ 150.5, 144.1, 143.4, 136.1, 134.3, 129.6, 125.4, 124.5, 121.9, 28.55, 15.19. Anal. Calcd for $C_{11}H_{10}BrN$: C, 55.96; H, 4.27; N, 5.93. Found: C, 55.88; H, 4.01; N, 5.93.

8-Bromo-6-*tert*-butylquinoline (1b). The same procedure as given above was used, using 2-bromo-4-*tert*-butylaniline as the starting material. **1b** was obtained as a colorless solid in 70% yield. ^{1}H NMR ($CDCl_3$, 400 MHz, 25 °C): δ 8.97 (dd, ^3J = 4.5 Hz, ^4J = 1.5 Hz, 1H), 8.13 (dd, ^3J = 8.0 Hz, ^4J = 2.0 Hz, 1H), 8.10 (dd, ^3J = 8.0 Hz, ^4J = 2.0 Hz, 1H), 7.68 (s, 1H), 7.40 (dd, ^3J = 4.0 Hz, ^3J = 8.0 Hz, 1H), 1.40 (s, 9H). ^{13}C NMR ($CDCl_3$, 100 MHz, 25 °C): δ 150.8, 150.5, 144.0, 136.8, 132.4, 129.4, 124.6, 123.1, 122.0, 35.18, 31.27. Anal. Calcd for $C_{13}H_{14}BrN$: C, 59.11; H, 5.34; N, 5.30. Found: C, 58.75; H, 5.22; N, 5.39.

8-Bromo-6-(trifluoromethoxy)quinoline (1c). The same procedure as given above was used, using 2-bromo-4-(trifluoromethoxy)aniline as the starting material. **1c** was obtained as a colorless solid in 87% yield. ^{1}H NMR ($CDCl_3$, 400 MHz, 25 °C): δ 9.02 (dd, ^3J = 4.0 Hz, ^4J = 2.0 Hz, 1H), 8.13 (dd, ^3J = 8.4 Hz, ^4J = 1.6 Hz, 1H), 8.10 (d, ^4J = 2.4 Hz, 1H), 7.60 (s, 1H), 7.48 (dd, ^3J = 4.4 Hz, ^3J = 8.0 Hz, 1H). ^{13}C NMR ($CDCl_3$, 100 MHz, 25 °C): δ 151.8, 146.5, 144.0, 136.7, 129.1, 127.5, 126.6, 123.0, 120.7(q, $^1J_{C-F}$ = 258 Hz). ^{19}F NMR ($CDCl_3$, 376 MHz, 25 °C): δ −58.37. Anal. Calcd for $C_{10}H_5NOBrF_3$: C, 41.13; H, 1.73; N, 4.80. Found: C, 41.38; H, 1.53; N, 4.85.

Synthesis of 6-Ethyl-8-quinolineboronic Acid (2a). To a −78 °C solution of **1a** (2.36 g, 10 mmol, in 40 mL of THF) under argon was added 5.8 mL of PhLi (1.8 M in di-*n*-butyl ether, 10.5 mmol) over 5 min. After the reaction mixture was further stirred at −78 °C for 1 h, trimethylborate (4.4 mL, 40 mmol) was added slowly. The mixture was then warmed to ambient temperature, further stirred for 4 h, acidified with 3 M HCl (50 mL), and washed with Et_2O. The aqueous layer was then neutralized with 10% NaOH solution to give an off-white precipitate, which was collected via vacuum filtration and recrystallized from a mixture of acetone and hexanes to afford **2a** as a white solid (1.4 g, 70%). ^{1}H NMR (CD_3OD/D_2O, 300 MHz, 25 °C): δ 9.20 (dd, ^3J = 5.0 Hz, ^4J = 1.5 Hz, 1H), 8.35 (dd, ^3J = 8.1 Hz, ^4J = 1.5 Hz, 1H), 7.97 (d, ^4J = 1.8 Hz, 1H), 7.62 (dd, ^3J = 5.1 Hz, ^3J = 8.0 Hz, 1H), 7.49 (s, 1H), 2.75 (q, ^3J = 7.5 Hz, 2H), 1.25 (t, ^3J = 7.5 Hz, 3H). ^{13}C NMR (CD_3OD/D_2O, 75 MHz, 25 °C): δ 144.6, 144.0, 142.4, 141.1, 134.9, 134.6, 129.7, 124.2, 120.3, 28.67, 14.38. ESI-MS: *m/z* calcd for $C_{11}H_{12}BNO_2$ 201.2, found 202.2 $[M + H]^+$.

(8) Lee, S. H.; Jang, B.; Kafafi, Z. H. *J. Am. Chem. Soc.* **2005**, *127*, 9071–9078.

(9) (a) Hill, G. S.; Irwin, M. J.; Levy, C. J.; Rendina, L. M.; Puddephatt, R. J. *Inorg. Synth.* **1998**, *32*, 149–153. (b) Song, D.; Wang, S. *J. Organomet. Chem.* **2002**, *648*, 302–305.

Table 1. Crystallographic Data

	1b	**1c**	**2b** solvate[a]	**3a**·$2CH_2Cl_2$	**3b**·$2CH_2Cl_2$	**3c**·$2CH_2Cl_2$
formula	$C_{13}H_{14}BrN$	$C_{10}H_5BrF_3NO$	$C_{27.70}H_{35.37}B_2N_2O_{4.20}$	$C_{52}H_{46}Cl_4N_4$	$C_{60}H_{62}Cl_4N_4$	$C_{48}H_{26}Cl_4F_{12}N_4O_4$
fw	264.16	292.06	485.17	868.73	980.94	1092.53
T (K)	150(2)	150(2)	150(2)	100(2)	150(2)	150(2)
space group	$P2_1/c$	$P2_1/n$	$C2/c$	$P2_1/n$	$P\bar{1}$	$P\bar{1}$
a (Å)	10.7872(2)	4.4543(4)	24.3205(6)	12.5079(3)	12.7286(4)	11.0134(4)
b (Å)	9.4647(3)	11.6713(16)	21.1932(5)	21.9598(9)	15.2208(6)	12.9399(7)
c (Å)	12.7521(3)	18.635(2)	34.2425(6)	19.3280(7)	15.4805(5)	17.9995(8)
α (deg)	90	90	90	90	104.520(2)	91.364(2)
β (deg)	110.5474(15)	94.179(7)	93.8930(10)	91.434(2)	105.413(2)	97.888(3)
γ (deg)	90	90	90	90	99.820(2)	103.432(3)
V (Å^3)	1219.13(5)	966.21(19)	17608.9(7)	5307.2(3)	2707.06(16)	2467.25(19)
Z	4	4	24	4	2	2
D_c (g cm^{-3})	1.439	2.008	1.098	1.087	1.203	1.471
μ (mm^{-1})	3.339	4.274	0.072	0.258	0.260	0.333
no. of rflns collected	9239	4710	68559	29692	30579	25236
no. of indep rflns	2135	1660	15478	9301	9504	11145
GOF on F^2	1.049	1.048	1.057	1.019	1.024	1.074
R ($I > 2\sigma(I)$)	$R_1 = 0.0381$	$R_1 = 0.0782$	$R_1 = 0.0686$	$R_1 = 0.0797$	$R_1 = 0.0633$	$R_1 = 0.0813$
	$wR_2 = 0.0913$	$wR_2 = 0.1993$	$wR_2 = 0.1719$	$wR_2 = 0.1654$	$wR_2 = 0.1515$	$wR_2 = 0.1921$
R (all data)	$R_1 = 0.0436$	$R_1 = 0.0981$	$R_1 = 0.1071$	$R_1 = 0.1340$	$R_1 = 0.1054$	$R_1 = 0.1556$
	$wR_2 = 0.0952$	$wR_2 = 0.2200$	$wR_2 = 0.1847$	$wR_2 = 0.1809$	$wR_2 = 0.1824$	$wR_2 = 0.2150$

	3d·$2.5C_7H_8$	**4b**	**5a**·$2CHCl_3$	**5b**·$2CHCl_3$	**5c**·$3CHCl_3$
formula	$C_{85.5}H_{80}Br_2N_2P_2Pd_2$	$C_{62}H_{70}N_4Pt_2$	$C_{56}H_{56}Cl_8N_4Pt_2$	$C_{64}H_{72}Cl_8N_4Pt_2$	$C_{53}H_{37}Cl_{11}F_{12}N_4O_4Pt_2$
fw	1570.07	1261.40	1458.83	1571.04	1802.00
T (K)	150(2)	150(2)	150(2)	150(2)	150(2)
space group	$P\bar{1}$	$P2_1/n$	$P\bar{1}$	$P\bar{1}$	$P\bar{1}$
a (Å)	14.1247(3)	16.0011(11)	9.3132(4)	10.0472(5)	11.2692(7)
b (Å)	15.4594(4)	11.9023(8)	11.8742(4)	12.0539(7)	12.5803(11)
c (Å)	19.5620(5)	17.1940(13)	13.3219(3)	13.3550(7)	12.6285(11)
α (deg)	82.4328(14)	90	67.5142(17)	70.392(2)	69.421(3)
β (deg)	72.3137(15)	101.730(3)	85.269(2)	83.136(4)	77.399(5)
γ (deg)	66.3941(14)	90	85.9551(17)	86.422(3)	84.709(5)
V (Å^3)	3728.86(16)	3206.2(4)	1355.37(8)	1512.25(14)	1635.5(2)
Z	2	2	1	1	1
D_c (g cm^{-3})	1.398	1.307	1.787	1.725	1.830
μ (mm^{-1})	1.642	4.394	5.591	5.018	4.801
no. of rflns collected	40214	22888	14282	18904	12861
no. of indep rflns	13104	5596	5880	6810	5643
GOF on F^2	1.065	1.043	1.080	0.992	1.070
R ($I > 2\sigma(I)$)	R1 = 0.0654	R1 = 0.0668	R1 = 0.0389	R1 = 0.0738	R1 = 0.0618
	wR2 = 0.1473	wR2 = 0.1578	wR2 = 0.0964	wR2 = 0.1600	wR2 = 0.1605
R (all data)	R1 = 0.1156	R1 = 0.0902	R1 = 0.0455	R1 = 0.1389	R1 = 0.0753
	wR2 = 0.1658	wR2 = 0.1710	wR2 = 0.1011	wR2 = 0.1917	wR2 = 0.1714

[a] Solvate 0.117 C_6H_{14}, 0.333 C_3H_6O, 0.867 H_2O.

Table 2. Selected Bond Lengths (Å) and Angles (deg)[a]

4b		**5a**		**5b**		**5c**	
Pt(1)−C(31)	2.014(14)	Pt(1)−C(27)	2.047(6)	Pt(1)−C(30)	2.043(12)	Pt(1)−C(24)	2.046(10)
Pt(1)−C(30)	2.046(11)	Pt(1)−C(26)	2.068(5)	Pt(1)−C(31)	2.053(11)	Pt(1)−C(25)	2.057(10)
Pt(1)−N(1)	2.134(8)	Pt(1)−C(24)	2.121(5)	Pt(1)−N(2)	2.157(9)	Pt(1)−N(1)	2.09(2)
Pt(1)−N(2)	2.145(9)	Pt(1)−N(1)	2.150(4)	Pt(1)−C(27)	2.161(11)	Pt(1)−C(22)	2.107(9)
C(27)−C(28)	1.404(13)	Pt(1)−N(2)	2.195(4)	Pt(1)−N(1)	2.191(9)	Pt(1)−N(2)	2.189(8)
C(28)−C(29)	1.375(16)	Pt(1)−Cl(1)	2.4562(13)	Pt(1)−Cl(1)	2.479(3)	Pt(1)−Cl(1)	2.455(3)
C(29)−C(27)#1	1.383(15)	C(23)−C(25)#2	1.337(7)	C(28)−C(29)	1.331(15)	C(21)−C(23)#4	1.318(13)
C(31)−Pt(1)−C(30)	88.4(5)	C(23)−C(24)	1.494(6)	C(27)−C(28)	1.500(15)	C(21)−C(22)	1.507(12)
C(31)−Pt(1)−N(1)	90.4(5)	C(24)−C(25)	1.496(6)	C(27)−C(29)#3	1.474(15)	C(22)−C(23)	1.489(13)
C(30)−Pt(1)−N(1)	177.9(4)	C(23)−C(24)−C(25)	112.5(4)	C(29)#3−C(27)−C(28)	114.3(9)	C(23)−C(22)−C(21)	112.3(8)
C(31)−Pt(1)−N(2)	173.7(4)	C(23)−C(24)−C(8)	112.8(4)	C(29)#3−C(27)−C(8)	108.0(9)	C(23)−C(22)−C(8)	106.5(7)
C(30)−Pt(1)−N(2)	87.3(4)	C(25)−C(24)−C(8)	106.0(4)	C(28)−C(27)−C(8)	112.6(8)	C(21)−C(22)−C(8)	113.9(7)
N(1)−Pt(1)−N(2)	93.8(3)	C(23)−C(24)−Pt(1)	109.8(3)	C(29)#3−C(27)−Pt(1)	110.1(7)	C(23)−C(22)−Pt(1)	111.0(6)
C(29)#1−C(27)−C(28)	117.6(10)	C(25)−C(24)−Pt(1)	111.0(3)	C(28)−C(27)−Pt(1)	108.5(7)	C(21)−C(22)−Pt(1)	109.2(6)
C(29)−C(28)−C(27)	119.3(9)	C(8)−C(24)−Pt(1)	104.4(3)	C(8)−C(27)−Pt(1)	102.7(7)	C(8)−C(22)−Pt(1)	103.6(6)
C(28)−C(29)−C(27)#1	123.1(10)						

[a] Legend: (#1) $2-x, -1-y, -z$; (#2) $1-x, -y, 1-z$; (#3) $-x, -y, -z$; (#4) $1-x, 2-y, -z$.

Synthesis of 6-*tert*-Butyl-8-quinolineboronic Acid (2b). The same procedure as above was used, using **1b** as the starting material (yield 50%). ^{1}H NMR (CD_3OD/D_2O, 300 MHz, 25 °C): δ 9.19 (d, ^3J = 3.9 Hz, 1H), 8.40 (d, ^3J = 8.1 Hz, 1H), 8.21 (d, ^4J = 2.1 Hz, 1H), 7.64 (d, ^4J = 2.1 Hz, 1H), 7.61 (d, J = 2.1 Hz, 1H), 1.26 (s, 9H). ^{13}C NMR (CD_3OD/D_2O, 75 MHz, 25 °C): δ 151.2, 143.8, 142.4, 142.0, 132.8, 132.6, 129.4, 121.8, 120.4, 34.72, 30.21. ESI-MS: m/z calcd for $C_{13}H_{16}BNO_2$ 229.2, found 230.2 [M + H]$^+$, 463.3 [2M − H_2O + Na]$^+$.

Synthesis of 6-(Trifluoromethoxy)-8-quinolineboronic Acid (2c). The same procedure as given above was used, using **1c** as the starting material (yield 55%). ^{1}H NMR (CD_3OD/D_2O, 300 MHz, 25 °C): δ 9.34 (dd, ^3J = 5.1 Hz, ^4J = 1.5 Hz, 1H), 8.58 (d, ^3J = 8.4 Hz, 1H), 7.95 (d, ^4J = 2.4 Hz, 1H), 7.79 (dd, ^3J = 5.0 Hz, ^3J

Scheme 3. Syntheses of 1a−c

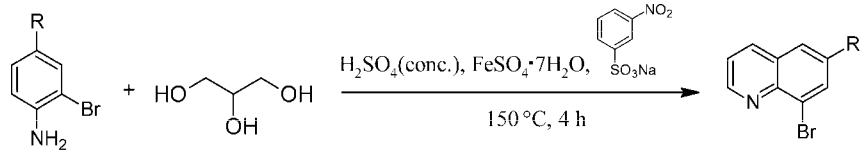

R = Et (**1a**), ^{t}Bu (**1b**), OCF_3 (**1c**)

Scheme 4. Syntheses of 2a−c

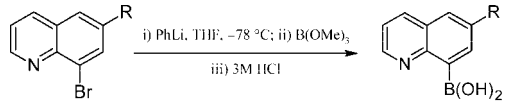

R = Et (**2a**), ^{t}Bu (**2b**), OCF_3 (**2c**)

Table 3. Selected ^{1}H NMR Data for 5a−c and $Pt_2Me_4Cl_2$(ttab)

	δ	$^2J_{Pt-H}$ (Hz)	$^3J_{Pt-H}$ (Hz)	$^4J_{Pt-H}$ (Hz)
5a	1.20	72.0		
	2.03	72.0		
	6.69		32	19.6
5b	1.02	72.0		
	2.20	74.0		
	6.79		32.8	20.8
5c	1.22	72.0		
	1.97	72.0		
	6.55		30.8	16.4
$Pt_2Me_4Cl_2$(ttab)	1.45	70.2		
	1.85	73.2		
	6.23		29.7[a]	14.7[a]

[a] The $^3J_{Pt-H}$ and $^4J_{Pt-H}$ coupling constants were misreported in the original paper[6] as 22.2 and 7.5 Hz, respectively.

= 8.0 Hz, 1H), 7.61 (d, ^4J = 2.1 Hz, 1H). ^{13}C NMR (CD_3OD/D_2O, 75 MHz, 25 °C): δ 148.3, 148.2, 144.5, 143.2, 142.4, 130.4, 126.7, 122.0, 120.7(q, $^1J_{C-F}$ = 256 Hz), 116.4. ^{19}F NMR (CD_3OD/D_2O, 282 MHz, 25 °C): δ −59.57. ESI-MS: *m*/*z* calcd for $C_{10}H_7BNO_3F_3$ 257.2, found 258.2 $[M + H]^+$, 519.2 $[2M - H_2O + Na]^+$.

Synthesis of 1,2,4,5-Tetrakis(6-ethylquinolin-8-yl)benzene (3a). A mixture of $Pd(PPh_3)_4$ (0.23 g, 0.2 mmol), 1,2,4,5-tetrabromobenzene (0.39 g, 1 mmol), **2a** (1.2 g, 6 mmol), and K_3PO_4 (10.7 g, 50 mmol) was placed in a Schlenk flask under argon. Degassed DMF (20 mL) and H_2O (20 mL) were added to the mixture, and the flask was heated to 95 °C under argon for 24 h. The mixture was then cooled down and partitioned by CH_2Cl_2 and water, and the aqueous layer was washed with CH_2Cl_2 several times. The organic layers were combined together and dried over Na_2SO_4. After filtration, the solvent was removed under vacuum, and the remaining oil was separated through a silica gel column with THF/hexanes as eluent and recrystallized from CH_2Cl_2 to afford **3a** (0.2 g, 30% yield) as colorless crystals. ^{1}H NMR ($CDCl_3$, 400 MHz, 52 °C): δ 8.61 (s, 4H), 7.96 (s, 2H), 7.83 (dd, ^3J = 8.4 Hz, ^4J = 1.6 Hz, 4H), 7.53 (d, ^4J = 2.0 Hz, 4H), 7.22 (d, ^4J = 2.0 Hz, 4H), 7.83 (dd, ^3J = 8.0 Hz, ^3J = 4.0 Hz, 4H), 2.52 (q, ^3J = 7.6 Hz, 8H), 0.96 (t, ^3J = 7.6 Hz, 12H). ^{13}C NMR ($CDCl_3$, 100 MHz, 52 °C): δ 148.6, 146.0, 141.8, 141.6, 138.6, 135.2, 134.9, 133.1, 128.4, 124.1, 120.2, 28.89, 15.22. Anal. Calcd for $C_{50}H_{42}N_4 \cdot 0.25CH_2Cl_2$: C, 83.81; H, 5.94; N, 7.78. Found: C, 83.49; H, 6.46; N, 7.95.

Synthesis of 1,2,4,5-Tetrakis(6-*tert*-butylquinolin-8-yl)benzene (3b). The same procedure as given above was used, using **2b** as the starting material (yield 35%). ^{1}H NMR ($CDCl_3$, 400 MHz, 52 °C): δ 8.64 (s, 4H), 8.06 (s, 2H), 7.88 (d, ^3J = 8.4 Hz, 4H), 7.68 (s, 4H), 7.38 (s, 4H), 7.13 (dd, ^3J = 7.2 Hz, ^3J = 3.6 Hz, 4H), 1.07 (s, 36H). ^{13}C NMR ($CDCl_3$, 100 MHz, 52 °C): δ 148.9, 148.5, 145.8, 141.4, 138.6, 135.8, 135.5, 131.3, 128.3, 121.5, 120.2, 34.76, 31.14. Anal. Calcd for $C_{58}H_{58}N_4 \cdot 2CH_2Cl_2$: C, 73.46; H, 6.37; N, 5.71. Found: C, 73.61; H, 6.24; N, 5.75.

Synthesis of 1,2,4,5-Tetrakis(6-(trifluoromethoxy)quinolin-8-yl)benzene (3c). The same procedure as given above was used, using **2c** as the starting material (yield 25%). ^{1}H NMR ($CDCl_3$, 400 MHz, 52 °C): δ 8.64 (s, 4H), 7.99 (s, 2H), 7.92 (d, ^3J = 8.0 Hz, 4H), 7.57 (s, 4H), 7.35 (s, 4H), 7.22 (dd, ^3J = 8.0 Hz, ^3J = 4.0 Hz, 4H). ^{13}C NMR ($CDCl_3$, 100 MHz, 52 °C): δ 150.0, 146.4, 145.0, 143.7, 138.0, 135.6, 135.2, 128.6, 125.6, 121.5, 120.7 (q, $^1J_{F-C}$ = 256 Hz), 117.3. ^{19}F NMR ($CDCl_3$, 376 MHz, 25 °C): δ −58.49. Anal. Calcd for $C_{46}H_{22}N_4F_{12}O_4 \cdot 0.25CH_2Cl_2$: C, 58.85; H, 2.40; N, 5.94. Found: C, 59.20; H, 2.53; N, 6.00.

Synthesis of [Pt_2Me_2(3a)] (4a). To a solution of $[PtMe_2(SMe_2)]_2$ (57.4 mg, 0.01 mmol, in 0.2 mL of THF and 4 mL of Et_2O) was added a solution of **3a** (70 mg, 0.01 mmol, in 2 mL of THF) slowly under argon. The mixture was stirred for 4 h at ambient temperature. The red precipitate was collected by vacuum filtration, washed with THF, and then dried under vacuum to afford **4a** as a red powder (97 mg, 85% yield). Anal. Calcd for $C_{54}H_{54}N_4Pt_2$: C, 56.44; H, 4.74; N, 4.88. Found: C, 56.35; H, 4.62; N, 4.93.

Synthesis of [Pt_2Me_2(3b)] (4b). The same procedure as given above was used, using **3b** as the starting material (yield 87%). Anal. Calcd for $C_{62}H_{70}N_4Pt_2$: C, 59.03; H, 5.59; N, 4.44. Found: C, 59.14; H, 5.40; N, 4.38.

Synthesis of [Pt_2Me_2(3c)] (4c). The same procedure as given above was used, using **3c** as the starting material (yield 75%). Anal. Calcd for $C_{50}H_{34}N_4O_4F_{12}Pt_2 \cdot$THF: C, 44.88; H, 2.93; N, 3.88. Found: C, 44.71; H, 3.02; N, 3.90.

Reaction of 4a with $CHCl_3$. A solution of **4a** (49 mg, 0.005 mmol) in 2 mL of $CHCl_3$ was stirred for 3 h at ambient temperature. The resulting yellow solution was dried under vacuum to afford **5a** as a yellow powder (57 mg, 95% yield). ^{1}H NMR ($CDCl_3$, 400 MHz, 25 °C): δ 9.75 (d, ^3J = 5.0 Hz, 2H), 9.69 (d, ^3J = 5.0 Hz, 2H), 8.61 (s, 2H), 8.18 (d, ^3J = 7.2 Hz, 2H), 7.93 (d, J = 6.4 Hz, 2H), 7.67 (s, 2H), 7.62 (dd, ^3J = 4.5 Hz, ^3J = 8.0 Hz, 2H), 7.52 (s, 2H), 7.39 (s, 2H), 7.02 (dd, ^3J = 4.5 Hz, ^3J = 8.0 Hz, 2H), 6.69 (s, satellite, $^3J_{Pt-H}$ = 32 Hz, $^4J_{Pt-H}$ = 19.6 Hz, 2H), 2.78−2.74 (m, 4H), 2.61−2.55 (m, 4H), 2.03 (s, satellite, $^2J_{Pt-H}$ = 72 Hz, 6H), 1.28 (t, ^3J = 7.6 Hz, 6H), 1.20 (s, satellite, $^2J_{Pt-H}$ = 72 Hz, 6H), 1.06 (t, ^3J = 7.6 Hz, 6H). Anal. Calcd for $C_{54}H_{54}N_4Cl_2Pt_2 \cdot 0.5CCl_3$: C, 51.15; H, 4.29; N, 4.38. Found: C, 51.25; H, 4.04; N, 4.33.

Reaction of 4b with $CHCl_3$. The same procedure as given above was used, using **4b** as the starting material to afford **5b** as a yellow powder (yield 94%). ^{1}H NMR ($CDCl_3$, 400 MHz, 25 °C): δ 9.77 (dd, ^3J = 4.8 Hz, ^4J = 1.6 Hz, 2H), 9.63 (dd, ^3J = 5.2 Hz, ^4J = 2.0 Hz, 2H), 8.97 (d, ^4J = 2.0 Hz, 2H), 8.22 (dd, ^3J = 8.4 Hz, ^4J = 1.6 Hz, 2H), 7.92 (dd, ^3J = 8.0 Hz, ^4J = 1.6 Hz, 2H), 7.84 (d, ^4J = 1.6 Hz, 2H), 7.64 (dd, ^3J = 4.8 Hz, ^3J = 8.0 Hz, 2H), 7.49 (d, ^4J = 2.0 Hz, 2H), 7.35 (d, ^4J = 2.0 Hz, 2H), 6.97 (dd, ^3J = 4.8 Hz, ^3J = 8.0 Hz, 2H), 6.79 (s, satellite, $^3J_{Pt-H}$ = 32.8 Hz, $^4J_{Pt-H}$ = 20.8 Hz, 2H), 2.20 (s, satellite, $^2J_{Pt-H}$ = 74 Hz, 6H), 1.36 (s, 18H), 1.02 (s, satellite, $^2J_{Pt-H}$ = 72 Hz, 6H), 1.10 (s, 18H). Anal. Calcd for $C_{62}H_{70}N_4Cl_2Pt_2 \cdot 0.25CCl_3$: C, 54.84; H, 5.30; N, 4.18. Found: C, 55.20; H, 5.36; N, 4.13.

Reaction of 4c with $CHCl_3$. The same procedure as given above was used, using **4c** as the starting material to afford **5c** as a yellow powder (yield 90%). ^{1}H NMR ($CDCl_3$, 400 MHz, 25 °C): δ 10.25 (d, ^3J = 4.8 Hz, 2H), 9.20 (d, ^3J = 5.2 Hz, 2H), 8.46 (s, 2H), 8.23 (d, ^3J = 8.0 Hz, 2H), 8.07 (d, ^3J = 8.0 Hz, 2H), 7.72 (dd, ^3J = 4.8 Hz, ^3J = 8.6 Hz, 2H), 7.68 (s, 2H), 7.48 (s, 2H), 7.36 (s, 2H), 7.23

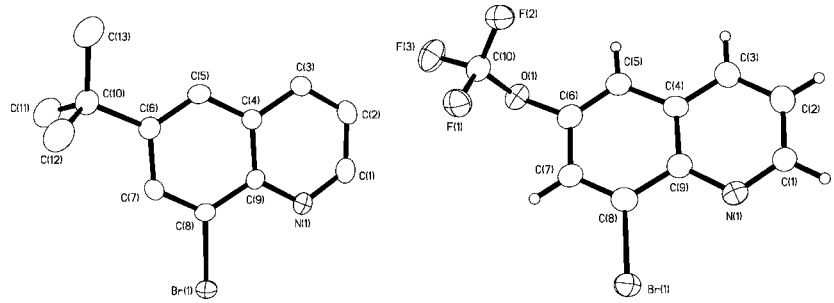

Figure 1. Molecular structures of **1b** (left) and **1c** (right) with thermal ellipsoids plotted at the 50% probability level.

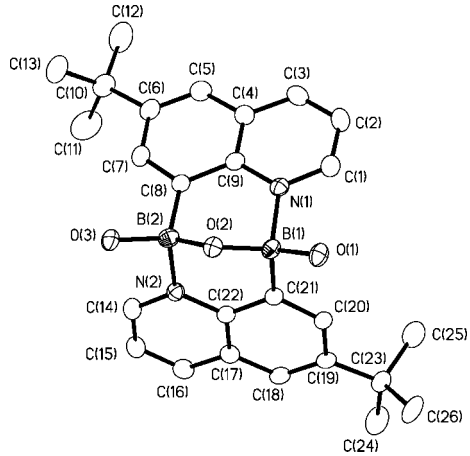

Figure 2. Molecular structure of **2b** in a dimeric form with the thermal ellipsoids plotted at the 50% probability level. All hydrogen atoms are removed for clarity.

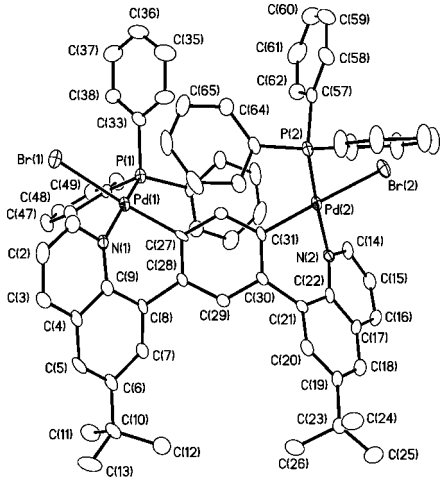

Figure 3. Molecular structure of **3d** with thermal ellipsoids plotted at the 50% probability level.

(dd, ^3J = 5.2 Hz, ^3J = 8.4 Hz, 2H), 6.55 (s, satellite, $^3J_{Pt-H}$ = 30.8 Hz, $^4J_{Pt-H}$ = 16.4 Hz, 2H), 1.97 (s, satellite, $^2J_{Pt-H}$ = 72 Hz, 6H), 1.22 (s, satellite, $^2J_{Pt-H}$ = 72 Hz, 6H). ^{19}F NMR ($CDCl_3$, 376 MHz, 25 °C): δ −58.21, −58.29. Anal. Calcd for $C_{50}H_{34}N_4Cl_2F_{12}Pt_2 \cdot 0.5CCl_3$: C, 40.34; H, 2.31; N, 3.73. Found: C, 40.07; H, 2.12; N, 4.00.

X-ray Diffraction Analyses. X-ray-quality crystals of **1b**,**c** and **3a**−**c** were obtained by top-layering the CH_2Cl_2 solutions with hexanes, those of **2b** were obtained by diffusing hexanes into a wet acetone solution, those of **3d** were obtained by top-layering a CH_2Cl_2 solution with toluene, those of **4b** were obtained by top-layering the CH_2Cl_2 solution with benzene, and those of **5a**−**c** were obtained by slow evaporation of the $CHCl_3$ solutions. All crystals were mounted on the tip of a MiTeGen MicroMount. The single-crystal X-ray diffraction data of **2b** were collected on a Bruker Kappa Apex II diffractometer, while all the remaining data were collected on a Nonius Kappa-CCD diffractometer. All data were collected with graphite-monochromated Mo Kα radiation (λ = 0.710 73 Å), at 50 kV and 30 mA, at a temperature of 150 K controlled by an Oxford Cryostream 700 series low-temperature system, except for the data of **3a**, which were collected at 100 K. The diffraction data of **2b** were processed with the Bruker Apex 2 software package,[10] while all the remaining data were processed with the DENZO-SMN package.[11] All structures were solved by the direct methods and refined using SHELXTL V6.10.[12] Compounds **1b**,**c** crystallized in the monoclinic space groups $P2_1/c$ and $P2_1/n$, respectively, with 1 molecule per asymmetric unit. **2b** crystallized in the monoclinic space group $C2/c$ with 3 independent molecules per asymmetric unit along with 1 acetone molecule, 0.35 *n*-hexane molecule, and 2.6 water molecules. **3a** crystallized in the monoclinic space group $P2_1/n$ with 1 molecule per asymmetric unit along with 2 molecules of CH_2Cl_2. **3b**,**c** crystallized in the triclinic space group $P\bar{1}$ with 1 molecule per asymmetric unit along with 2 molecules of CH_2Cl_2. **3d** crystallized in the triclinic space group $P\bar{1}$ with 1 molecule per asymmetric unit along with 2.5 toluene molecules. **4b** crystallized in the monoclinic space group $P2_1/n$ with 0.5 molecule per asymmetric unit. **5a**−**c** crystallized in the triclinic space group $P\bar{1}$ with 0.5 molecule per asymmetric unit along with 2 (for **5a**,**b**) or 3 (for **5c**) molecules of $CHCl_3$. The disordered *tert*-butyl groups in **2b** and **3b**, a cocrystallized toluene molecule in **3d**, the quinolinyl groups and OCF_3 groups in **5c**, and cocrystallized $CHCl_3$ molecules in the lattice of **5c** were modeled successfully. The residual electron density from disordered, unidentified solvent molecules in the lattices of **2b**, **3a**,**c**,**d,** and **4b** were removed with the SQUEEZE function of the PLATON program,[13] and their contributions were not included in the formula. All non-hydrogen atoms were refined anisotropically, except for the disordered portions. In all structures hydrogen atoms bonded to carbon atoms were included in calculated positions and treated as riding atoms. The positions of hydrogen atoms attached to oxygen atoms were calculated to fit the hydrogen bonding patterns. The crystallographic data are summarized in Table 1, while selected bond lengths and angles are given in Table 2.

Results and Discussion

Syntheses and Structures of Ligands 3a−c. The novel quinoline-based tetradentate ligands **3a**−**c** can be synthesized in three steps.

(10) Apex 2 Software Package; Bruker AXS Inc., 2008.
(11) Otwinowski, Z.; Minor, W. In *Macromolecular Crystallography, Part A*; Carter, C. W., Sweet, R. M., Eds.; Academic Press: London, 1997; Methods in Enzymology, Vol. 276, p 307.
(12) Sheldrick, G. M. *Acta Crystallogr., Sect. A: Found. Crystallogr.* **2008**, *64*, 112–122.
(13) Spek, A. L. *J. Appl. Crystallogr.* **2003**, *36*, 7.

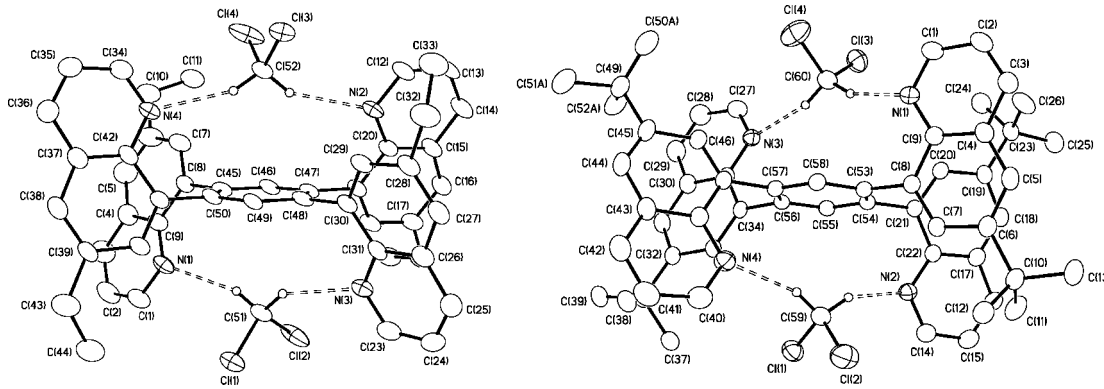

Figure 4. Molecular structures of **3a** (left) and **3b** (right) (both interacting with CH_2Cl_2 molecules) with thermal ellipsoids plotted at the 50% probability level. All hydrogen atoms (except for those of CH_2Cl_2 molecules) are omitted for clarity.

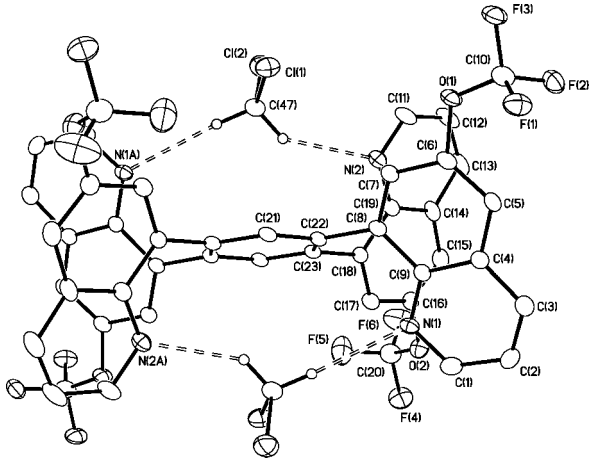

Figure 5. Molecular structure of **3c** (interacting with CH_2Cl_2 molecules) with thermal ellipsoids plotted at the 50% probability level. All hydrogen atoms (except for those in CH_2Cl_2 molecules) are omitted for clarity.

The first step is to build the 6-substituted 8-bromoquinolines **1a**−**c**, through modified Skraup reactions (Scheme 3),[14] using appropriate para-substituted 2-bromoanilines as the starting materials. Compound **1a** was obtained as a pale yellow oil in 60% yield, while **1b**,**c** were obtained as white solids in 70 and 87% yields, respectively. All three compounds have been characterized by NMR spectroscopy and elemental analysis, while the structures of **1b**,**c** have also been confirmed by X-ray crystallography and shown in Figure 1.

The second step is to convert **1a**−**c** into the corresponding boronic acids for the subsequent Suzuki coupling reactions. Boronic acids **2a**−**c** can be obtained in 50−70% yield from the reactions of **1a**−**c** and phenyllithium at −78 °C in THF, followed by sequential treatments with trimethylborate and 3 M HCl (Scheme 4). The use of *n*-butyllithium instead of phenyllithium can also lead to the formation of the desired products, but the reactions have lower yields.

It is well-known that boronic acids can undergo intermolecular condensation to form oligomers, losing water molecules.[15] Thus, the existence of **2a**−**c** depends on their hydration states; in most cases, species of different hydration states coexist. For example, the ^1H NMR of the vacuum-dried boronic acid **2b** is messy in CD_3COCD_3 or CD_3OD; however, by adding one drop of D_2O to the NMR solution, the spectrum shows only one set of signals which could be attributed to the fully hydrated form, the monomer.

When **2b** is recrystallized from wet acetone and hexanes, X-ray crystallography reveals a novel dimeric structure, which is shown in Figure 2. Each boron center has a tetrahedral geometry with a terminal OH group, a bridging oxo, a nitrogen atom from one quinoline moiety, and a carbon atom from the other quinoline moiety occupying the four vertices. In the crystal lattice, molecules of **2b** form multiple intermolecular hydrogen bonds with one another as well as the lattice water molecules. The MS spectrum of as-synthesized **2b** shows the presence of both the monomer and the dimer. Because of the coexistence of different forms, no satisfactory elemental analysis results could be obtained for the boronic acids **2a**−**c**. The as-synthesized **2a**−**c** were used in large excess without further purification in the subsequent Suzuki coupling reactions.[16] Because the Suzuki coupling reactions use water as a cosolvent at an elevated temperature, it is likely that different forms of these boronic acids convert to the fully hydrated monomer forms in the reaction system.

The tetradentate ligands **3a**−**c** can be obtained via Suzuki coupling reactions of the corresponding boronic acids **2a**−**c** and 1,2,4,5-tetrabromobenzene catalyzed by $Pd(PPh_3)_4$ in the presence of K_3PO_4 in the DMF/H_2O solvent system at 95 °C under argon (Scheme 5). The yields of **3a**−**c** can be increased slightly by using 1,2,4,5-tetraiodobenzene instead of 1,2,4,5-tetrabromobenzene. A number of byproducts, such as di- and trisubstituted coupling products, have been observed, whose structures have been confirmed by X-ray crystallography and are shown in Figures S1 and S2 (see the Supporting Information). Another byproduct isolated in small quantity from the reaction mixture of the synthesis of **3b** is the dinuclear Pd(II) complex **3d**, whose identity has been confirmed by X-ray crystallography. As shown in Figure 3, the molecule of **3d** has two 6-*tert*-butylquinoline moieties attached to the central benzene ring in a mutually meta fashion. Each nitrogen donor atom of the quinoline moiety coordinates to a square-planar Pd(II) center that is further bonded with a carbon donor atom of the central benzene ring, a bromide ligand trans to the carbon donor, and a PPh_3 ligand trans to the quinoline nitrogen atom. Compound **3d** is presumably a trapped intermediate of the Suzuki coupling reaction. After the coupling of the first two quinoline moieties to the central benzene ring, the two remaining C−Br bonds are oxidatively cleaved by the Pd(0) catalyst directed by the neighboring quinoline nitrogen

(14) Cohn, E. W. *J. Am. Chem. Soc.* **1930**, *52*, 3685–3688.

(15) Hall, D. G. *Boronic Acids: Preparation and Applications in Organic Synthesis and Medicine*; Wiley-VCH: Weinheim, Germany, 2005.

(16) Suzuki, A. *J. Organomet. Chem.* **1999**, *576*, 147–168.

Scheme 5. Synthesis of 3a−c

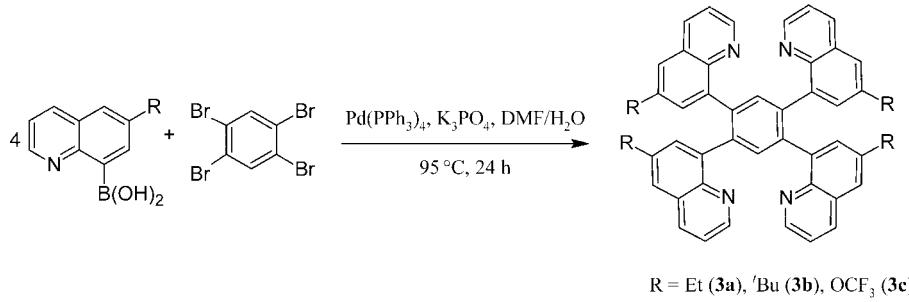

R = Et (**3a**), ^{t}Bu (**3b**), OCF_3 (**3c**)

Scheme 6. Syntheses of 4a−4c

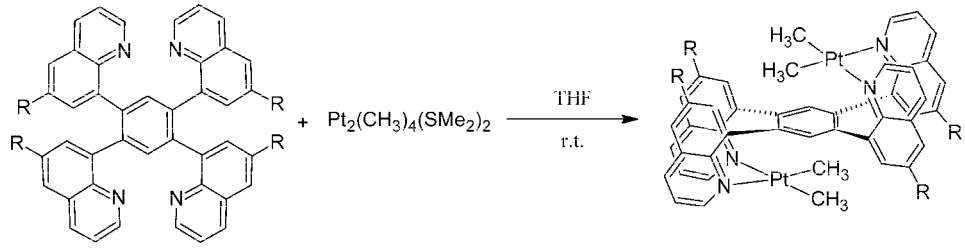

R = Et (**4a**), ^{t}Bu (**4b**), OCF_3 (**4c**)

Scheme 7. Syntheses of 5a−c

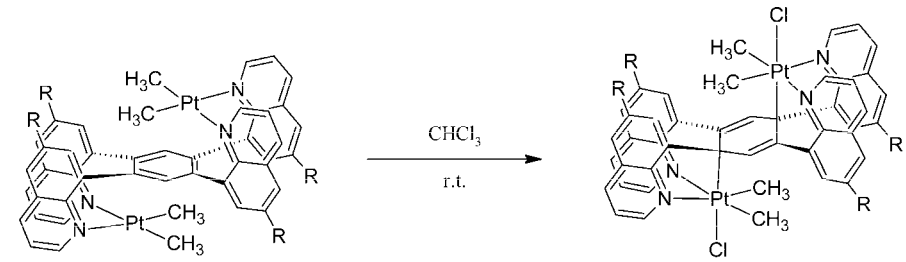

R = Et (**5a**), ^{t}Bu (**5b**), OCF_3 (**5c**)

atoms. Interestingly, compound **3d** is sufficiently stable to survive the cross-coupling conditions and a silica gel column.

Ligands **3a−c** were characterized by NMR spectroscopic, elemental, and single-crystal X-ray diffraction analyses. The ^{1}H NMR spectra of these ligands in $CDCl_3$ show several broad peaks at ambient temperature, presumably as a result of hindered rotations, while the spectra recorded at 52 °C show sharp signals. The protons of the central phenyl rings in **3a−c** resonate at 7.96, 8.06, and 7.99 ppm, respectively, as singlets integrated for 2 protons each, while the protons of the quinolinyl moieties in each compound show 5 resonances in the aromatic region, integrated for 4 protons each. The ethyl groups of **3a** give rise to a quartet and triplet in the ^{1}H NMR spectrum at 2.52 and 0.96 ppm integrated for 8 and 12 protons, respectively, while the *tert*-butyl groups of **3b** show a singlet at 1.07 ppm integrated for 36 protons. The ^{19}F NMR spectrum of **3c** has only one singlet at −58.49 ppm. All these NMR data indicate symmetric structures of these tetradentate ligands.

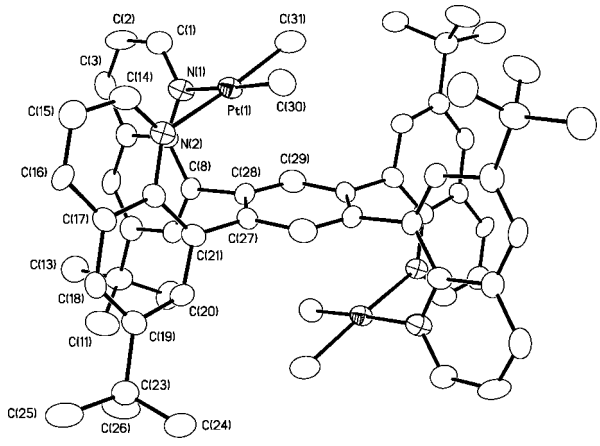

Figure 6. Molecular structure of **4b** with thermal ellipsoids plotted at the 50% probability level. All hydrogen atoms are omitted for clarity.

The molecular structures of **3a**,**b** are shown in Figure 4. In the structures of **3a**,**b**, each pair of mutually para quinoline moieties are of the same orientation (with nitrogen atoms on the same side of the central phenyl ring) and are different from the other pair. The dihedral angles between the central phenyl ring and the quinoline moieties are in the range of 70−76° for **3a** and 76−81° for **3b**, indicating that the quinoline moieties in **3b** are more perpendicular to the central phenyl ring. This is likely caused by the bulkier *tert*-butyl groups in **3b**, compared to the ethyl groups in **3a**. Each pair of nitrogen atoms on the same side of the central phenyl ring interacts with one CH_2Cl_2 molecule through nonclassic hydrogen bonds in a chelating fashion, with average N···C distances of ∼3.25 and ∼3.23 Å for **3a**,**b**, respectively. Such interactions may help lock down the motions of these ligands and, in turn, the crystallization.

The molecular structure of **3c** is shown in Figure 5. Unlike **3a**,**b**, each molecule of **3c** has a crystallographically imposed

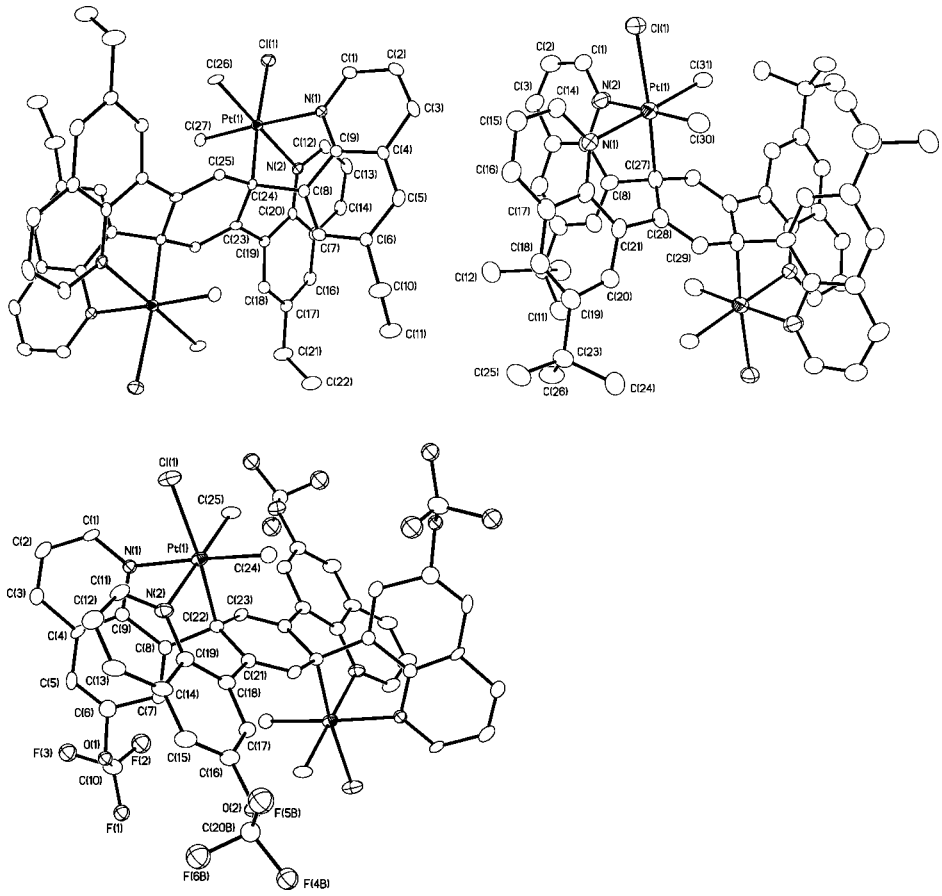

Figure 7. Molecular structures of **5a** (upper left), **5b** (upper right), and **5c** (bottom) with thermal ellipsoid plotted at the 30% probability level. All hydrogen atoms are omitted for clarity.

center of inversion at its centroid. As a consequence, each pair of mutually para quinoline moieties are of opposite orientations. Each pair of mutually meta quinoline moieties are of the same orientation, with the nitrogen atoms interacting with a CH_2Cl_2 solvent molecule through nonclassic hydrogen bonds in a chelating fashion, with an average N···C distance of ~3.37 Å. The dihedral angles between the central phenyl ring and the quinoline moieties are ~61 and ~65°, smaller than those found in **3a**,**b**, which could be the result of different H-bonding modes.

Syntheses and Structures of 4a−c. The dinuclear dimethylplatinum(II) complexes **4a−c** can be obtained as red precipitates by reacting **3a−c** with $[PtMe_2(Me_2S)]_2$ in THF at ambient temperature (Scheme 6). These complexes are stable in air at ambient temperature in the solid state. Although functionalized with ethyl, *tert*-butyl, and OCF_3 groups, complexes **4a−c** are sparingly soluble in common solvents (except for $CHCl_3$, which reacts with all three compounds); therefore, no NMR data have been obtained.

With the limited solubility of **4b** in CH_2Cl_2, X-ray-quality crystals were obtained by slow diffusion of benzene into a CH_2Cl_2 solution of **4b**. As shown in Figure 6, each molecule of **4b** has a crystallographically imposed center of inversion at its centroid. The **3b** ligand uses its nitrogen donor atoms from two quinolinyl groups that are mutually ortho to chelate to each square-planar platinum(II) center, with methyl ligands trans to the nitrogen donor atoms. The two platinum(II) centers are on the opposite sides of the central phenyl ring, with a short contact distance between Pt(1) and C(28) of 2.90(1) Å, shorter than the corresponding distance (3.11 Å) in $Pt_2Me_4(ttab)$[6] and the sum of the van der Waals radii of Pt and C (3.47 Å).[17] The intramolecular Pt···Pt distance in **4b** is 6.5626(9) Å, shorter than that (6.898(2) Å) in $Pt_2Me_4(ttab)$. The dihedral angle between the Pt(II) coordination plane and the central phenyl ring is ~27°, slightly smaller than that in $Pt_2Me_4(ttab)$. These observations are consistent with our ligand design (Scheme 2).

Reactivities of 4a−c with $CHCl_3$. The red compounds **4a−c** react with chloroform readily upon dissolution at ambient temperature to give the yellow products **5a−c**, respectively, in quantitative yield within 3 h (Scheme 7). Compounds **5a−c** have enough solubility for ^1H NMR spectroscopic analyses and are stable in the solid state and in solution at ambient temperature.

The selected ^1H NMR data for **5a−c** and $Pt_2Me_4Cl_2(ttab)$ are given in Table 3. Each compound (**5a−c**) has two singlets at 1.02−1.22 and 1.97−2.20 ppm with platinum satellites in the aliphatic regions, integrated for six protons each, which can be assigned to two types (two of each type) of methyl groups bonded to the platinum centers. These chemical shifts and the corresponding $^2J_{Pt-H}$ values are similar to those reported for $Pt_2Me_4Cl_2(ttab)$, except that the two methyl signals are slightly farther apart than those from $Pt_2Me_4Cl_2(ttab)$, indicating a greater difference between the two sets of methyl groups in **5a−c**. The protons of the central C_6 rings of **5a−c** resonate in the range of 6.55−6.79 ppm, more downfield than those of $Pt_2Me_4Cl_2(ttab)$. The characteristic platinum-satellite peaks indicate a bonding mode similar to that in $Pt_2Me_4Cl_2(ttab)$. The $^3J_{Pt-H}$ and $^4J_{Pt-H}$

(17) Emsley, J. *The Elements*, 2nd ed.; Clarendon Press: Oxford, U.K., 1991.

values of **5a**−**c** are in the ranges of 30.8−32.8 and 16.4−20.8 Hz, respectively, greater than those observed for $Pt_2Me_4Cl_2$-(ttab).

The structures of **5a**−**c** have been confirmed unambiguously by X-ray crystallography and are shown in Figure 7. All compounds possess crystallographically imposed inversion center symmetry. Each Pt(IV) center adopts a distorted-octahedral coordination geometry, with two nitrogen donor atoms from two quinolinyl groups, two methyl ligands, a chloride, and a carbon donor atom from the central C_6 ring of the tetradentate ligand occupying the six coordination sites, with bond lengths and angles similar to those in $Pt_2(CH_3)_4(ttab)Cl_2$.[6] Similar to the central C_6 ring in $Pt_2(CH_3)_4(ttab)Cl_2$, those of **5a**−**c** are planar with two CC double bonds (1.318(13)−1.337(7) Å) and four CC single bonds (1.474(15)−1.507(12) Å) in each ring, as indicated by the bond lengths.[17] The carbon atoms bonded to the metal centers have the typical sp^3 characters, with the average of bond angles around the carbon centers of 109.4° in all three cases (Table 2). The coordination spheres of the Pt(IV) centers in **5a**−**c** are similar to those in $PtClMe_2\{(pz)_2CRCH_2$-$\kappa N,N',C''\}$ (R = Me, CH_2Cl; pz = pyrazol-1-yl) compounds reported by Canty and co-workers:[18] i.e., two methyl ligands are trans to the nitrogen donor atoms of the NCN tripod ligand, while the chloride ligand is trans to an sp^3-hybridized carbon donor atom of the NCN tripod ligand.

Light appears to play no significant role in the reactions of **4a**−**c** with $CHCl_3$. Despite the shorter distances between the metal centers and the central phenyl rings in **4a**−**c** compared to that in $Pt_2Me_4(ttab)$, the reactions between **4a**−**c** and $CHCl_3$ are much slower than that between $Pt_2Me_4(ttab)$ and $CHCl_3$. The insolubility of **4a**−**c** makes it difficult to study the C−Cl activation reactions further. Further tuning on the ligand design is still necessary.

Conclusion

Three novel tetradentate ligands (**3a**−**c**) with quinoline functionalities have been designed and synthesized. As expected, the corresponding dinuclear dimethylplatinum(II) complexes structurally resemble the previously reported $Pt_2Me_2(ttab)$ compound. We have achieved a shorter distance between the metal center and the central phenyl ring of the ligand in comparison to that of $Pt_2Me_2(ttab)$ through proper ligand design. In addition to the structural similarity, complexes **4a**−**c** are also analogous to $Pt_2Me_2(ttab)$ in terms of reactivity toward C−Cl activation. Thus, they react with $CHCl_3$ under ambient conditions to afford **5a**−**c**, respectively. During these reactions, C−Cl bonds from $CHCl_3$ are cleaved, the Pt(II) centers are oxidized into Pt(IV), and the central phenyl rings of the tetradentate ligands are reduced into the corresponding planar cyclohexadiene dianions bonded to the Pt(IV) centers on both sides.

Although the Pt(II) compounds **4a**−**c** are much less soluble than $Pt_2Me_2(ttab)$, the Pt(IV) compounds **5a**−**c** appear to be more soluble than $Pt_2Me_2(ttab)Cl_2$ in common organic solvents. This may allow us to study the possible reduction of these Pt(IV) complexes back to the corresponding Pt(II) complexes. In addition, ligands with other functional groups might be able to solubilize both the Pt(II) and Pt(IV) compounds, which will allow extensive solution study on both the forward and backward reactions. The possibility of reducing **5a**−**c** back to **4a**−**c** and new ligands with solubilizing functional groups are being investigated in our laboratory.

Acknowledgment. This research is supported by grants to D.S. from the Natural Science and Engineering Research Council (NSERC) of Canada, the Canadian Foundation for Innovation, the Ontario Research Fund (ORF), and the University of Toronto (Connaught Foundation).

Supporting Information Available: CIF files giving crystallographic data for **1b**,**c**, **2b**, **3a**−**d**, **4b**, and **5a**−**c** and figures giving the molecular structures of the di- and trisubstituted byproducts from the synthesis of **3b**. This material is available free of charge via the Internet at http://pubs.acs.org.

OM800893R

(18) Canty, A. J.; Honeyman, R. T. *J. Organomet. Chem.* **1990**, *389*, 277–288.